RESEARCH DEPARTMENT

Spatial filtering applied to film printing: some fundamental considerations

RESEARCH REPORT No. PH-20

UDC 778. 58: 535. 421. 1968/41

THE BRITISH BROADCASTING CORPORATION
ENGINEERING DIVISION

RESEARCH DEPARTMENT

SPATIAL FILTERING APPLIED TO FILM PRINTING: SOME FUNDAMENTAL CONSIDERATIONS

Research Report No. PH-20
UDC 778.58: 1968/41
535.421

It uses SI units in accordance with B.S. document PD 5686.

A.H. Jones, B.Sc.

Head of Research and Development

Research Report No. PH-20

SPATIAL FILTERING APPLIED TO FILM PRINTING: SOME FUNDAMENTAL CONSIDERATIONS

August 1968

Research Report No. PH-20
UDC 778.58: 1968/41
535.421

SPATIAL FILTERING APPLIED TO FILM PRINTING: SOME FUNDAMENTAL CONSIDERATIONS

SUMMARY

Some of the fundamental properties of imaging systems using coherent illumination are discussed, and the basic technique of spatial filtering is described. A means whereby the technique might be extended to allow some compensation to be made for colour film printing losses is then proposed. Certain important fundamental and practical difficulties are incurred in such an arrangement, and these are carefully examined. Results of calculations and measurements made to date are given, and some general conclusions are drawn.

1. INTRODUCTION

The Fourier transforming property of optical systems, and its possible application using coherent light to the selective transmission of spatial information has been appreciated for many years. Several workers have given consideration to it as an aspect of the diffraction caused by the wave nature of light[1], but the first comprehensive mathematical treatment of the subject is generally attributed to Duffieux[2].

The basic principle may be explained simply as follows. The lens in Fig. 1 is being used to project on to the image plane the transparency shown on the left, whose illumination is supposed to come from a source of coherent light. A succession of plane wavefronts, defined by a series of planes at right angles to the arrows, will therefore approach the transparency, moving in the direction indicated by the arrows. As each wave passes through the transparency, its amplitude, which until this time had been constant over the wavefront, is modified to the variable transmission that exists over the surface of the transparency. The wave does not, however, remain in this modified form during the subsequent propagation, but immediately begins to separate into a number of plane waves moving at various angles to the optical axis. The directions of motion of a typical pair of wavefronts thus introduced by the transparency are shown in Fig. 1 by the dashed lines; these are rays proceeding from three arbitrarily chosen points within the transparency. Some of the original plane wave remains; its progress is indicated by the solid lines. The amplitudes and directions of this set of plane waves are considered in greater detail in Section 2.

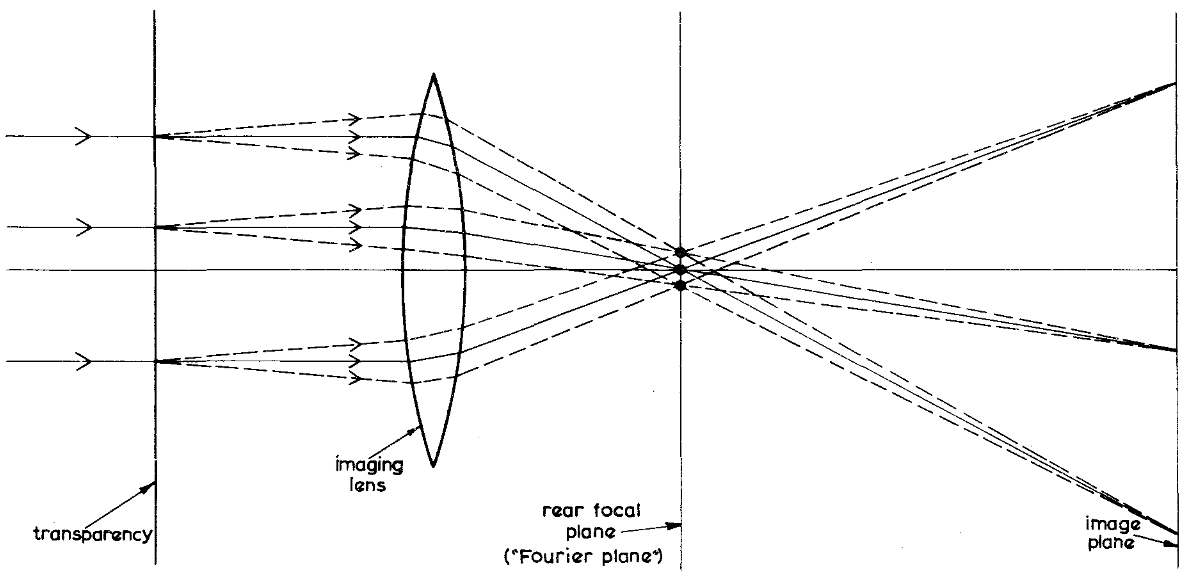

Fig. 1 - Diagram showing ray paths that occur when an image is formed by means of coherent light

The waves are then intercepted by the lens, which is here assumed to be free from aberrations. Each wavefront emerging from the lens has become spherical in shape, and now proceeds to converge upon a point of focus in the rear focal plane of the lens. It then diverges again and combines with similar wavefronts focused elsewhere in the rear focal plane to form the image. This latter part of the process will also be examined further in Section 2.

The position at which the above points of focus occur in the rear focal plane is a function of the direction in which the corresponding plane waves are moving as they enter the lens; the more these directions are inclined away from the main optical axis, the further from the axis will the focused points lie. The amplitude distribution in the focal plane may in fact be shown to be given by the two-dimensional Fourier transform of the amplitude distribution just to the right of the transparency – i.e. it is that of the original plane wave as modified by the transparency just before it breaks up to form the separately focused components. We therefore refer to the rear focal plane of the lens as the Fourier plane, and it contains a representation of the two-dimensional spectrum of the information carried by the light leaving the transparency.

It is now possible to modify the information contained in the image by putting into the Fourier plane an object which transmits some Fourier components with different attenuations or phase shifts from those given to other components. An axial aperture, for instance, will remove high-frequency components from the image, whilst an axial stop will remove the mean level (dc) and low-frequency components, and so on. An object inserted into the Fourier plane for this purpose is known as a spatial filter[3].

The development of the laser has made available relatively intense beams of coherent light, and this has stimulated a considerable interest in

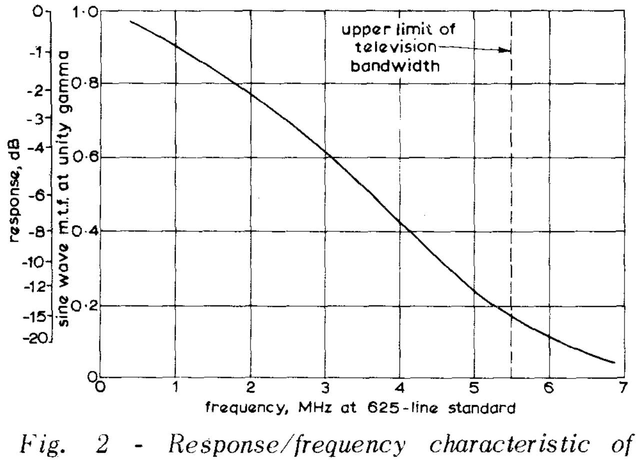

Fig. 2 - Response/frequency characteristic of typical colour film process involving 35-to-16 mm reduction printing

spatial filtering[4]. The technique has been used for the extraction of specific information and the suppression of unwanted detail from recorded data[5]. Spatial filtering has also been considered as a method of broad-band equalisation for the improvement of photographic printing[6], and a detailed investigation of this subject was made by Croce[7].

The present work is in some respects similar to that of Croce but differs from it in several important aspects. It was undertaken to find whether spatial filtering could profitably be applied to the production of 16 mm colour cine prints from 35 mm negative material. Fig. 2 shows the modulation transfer (response/frequency) characteristic of a typical colour film process involving a down-printing operation. 35 mm colour negative material was exposed to a series of black-and-white test bar patterns, developed, and then down-printed to produce a 16 mm positive print. Fig. 2 was derived from measurements (using broad-band illumination) of the depth of modulation present on the print*. It will be seen that at the spatial frequency corresponding to the limit of the television bandwidth an overall loss of about 15 dB has occurred. A typical black-and-white reduction printing process was found to cause a corresponding loss of 7 dB.

If the film were intended to be used for television, some correction for this loss of resolution could be provided within the telecine circuitry. It might for instance be effected by modifying the existing aperture correction circuits. This method however would improve resolution at the expense of signal-to-noise ratio. It was therefore thought that a more worthwhile improvement might be possible if spatial filtering were included in the optical printing process. One further advantage of spatial filtering would be that correction could easily be made in both the horizontal and the vertical directions; vertical aperture correction by electronic means, on the other hand, requires the use of at least one delay-line.

Much of the work to be described was influenced by an important practical consideration. It was thought that if spatial filtering were to be introduced it should entail the minimum of modification to existing printing machines. In particular, the use of lasers was excluded in this first investigation and the illumination was made sufficient to enable printing to be carried out at the normal speed (approximately twice the projection speed). These restrictions were found to have far reaching consequences affecting the feasibility of the arrangement originally envisaged.

In Section 2, some of the fundamental properties of imaging systems which use coherent or nearly coherent illumination will be further considered.

* This work was done by Mrs. G. Cleeve.

2. BASIC PRINCIPLES

This section describes in further detail the process by which a Fourier transform distribution is produced in the rear focal plane of the imaging lens, and then shows how the light leaving this plane produces the image. It is assumed unless otherwise stated that the transparency is illuminated by perfectly collimated light and that an image is formed by means of a hypothetical thin lens free from aberrations.

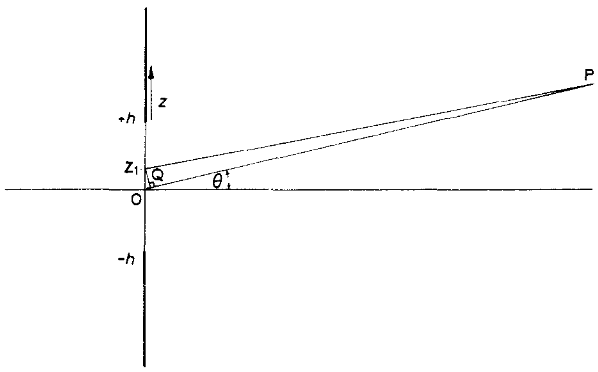

Fig. 3 - Diagram used in calculating propagation from transparency

2.1. The Formation of a Fourier Distribution

In Fig. 3 a cross section of the transparency is represented by the z axis. The upper and lower boundaries of the transparency are assumed to be at $z = \pm h$ and between these limits variation in transmission is assumed to take place in the z direction only. Therefore light approaching the transparency from the left and moving in the plane of the paper is deflected upwards or downwards within the plane of the paper. The amplitude transmission factor of the transparency is defined by $A(z)$. This distribution is impressed upon the amplitude of the wave as it passes through the transparency.

Consider the light emerging from a strip of transparency at right angles to the paper and of height dz positioned at Z_1. According to Huygen's principle the light leaving this strip may be considered to be radiated as a series of cylindrical waves of amplitude $A(Z_1)\mathrm{d}z$, the wavefronts being centred on Z_1. A similar train of waves of amplitude $A(\mathrm{O})\mathrm{d}z$ would be radiated from a strip centred at the origin O.

Now consider the amplitude measured at a point P and resulting from the radiation at Z_1. P is supposed to be so far away from the transparency that for $-h<z<+h$, Oz subtends a vanishingly small angle at P. Then if a perpendicular Z_1Q is dropped from Z_1 on to OP, the distance OQ = OZ_1 sinθ represents the path difference at P between radiation originating at Z_1 and radiation originating at O. If therefore the phase of the radiation at P received from Z_1 is expressed with respect to that from O, we have as the contribution at P due to Z_1 an amplitude

$$A(Z_1)e^{i(2\pi/\lambda)OZ_1 \sin\theta}dz$$

– neglecting a normalizing factor that takes into account an attenuation defined by the inverse square law.

Considering the complete transparency to be made up of a very large number of such strips, we obtain the total amplitude at P by integrating the incremental contributions defined above from $z = -h$ to $z = +h$, i.e. total amplitude at P is

$$A(\theta) = \int_{-h}^{+h} A(z)e^{i(2\pi/\lambda)z\sin\theta}dz$$

There is a clear similarity between this expression and the well-known Fourier transform relationship

$$A[\omega] = \int A(x)e^{-i\omega x}dx$$

where square brackets [] represent spectrum and parentheses () represent space function.

Now if P is sufficiently removed from the transparency, then in the region of P the individual cylindrical waves have effectively become plane and parallel, moving in the direction OP. Thus as P $\to \infty$ what we have calculated above as $A(\theta)$ is the amplitude of a plane wave at infinity which is inclined at an angle θ to the optical axis. Now if a convex lens is mounted so as to intercept the rays OP, Z_1P, etc., its axis being coincident with the optical axis, the above plane wave will be focused at a point lying within the rear focal plane of the lens and displaced from the axis by a distance $d = F \tan\theta \approx F.\theta$ if θ is small, F being the focal length.

Now suppose, to take a simple example, that the transparency is a sinusoidal grating pattern, the axes of the grating bars being at right angles to the paper in Fig. 3. Then $A(z)$ can be written

$A(z) = A(1 + a \cos kz)$, where a is the depth of modulation.

Then

$$A(\theta) = \int_{-h}^{h} Ae^{i\phi z}dz + \int_{-h}^{h} Aa \cos kz e^{i\phi z}dz$$

where $\phi = \dfrac{2\pi}{\lambda}\sin\theta$.

This may be shown to be equivalent to

$$A(\theta) = 2hA\frac{\sin\phi h}{\phi h} + ahA\frac{\sin(\phi + k)h}{(\phi + k)h} + ahA\frac{\sin(\phi - k)h}{(\phi - k)h}$$

The above expression clearly corresponds to a Fourier transformation of the amplitude distribution $A(z)$; we have a $(\sin x)/x$ distribution centred at $\phi = 0$, and two displaced $(\sin x)/x$ distributions centred at $\phi = \pm k$ respectively.

These displaced $(\sin x)/x$ distributions are reduced in amplitude in respect to the main one by the factor $a/2$, where $\phi = \pm k$, $\theta = \theta_k = \pm\sin^{-1}(k\lambda/2\pi)$. Since $k\lambda$ is small for the range of spatial frequencies considered, we may accurately write $\theta_k = \pm k\lambda/2\pi$. The corresponding displacement in the Fourier plane is therefore given by

$$d \approx F\theta_k = \pm F\lambda k/2\pi = \pm Ff\lambda$$

where $f = k/2\pi$ is the spatial frequency of the sinusoidal grating pattern.

If h is made sufficiently large, the above $(\sin x)/x$ distributions that comprise $A(\theta)$ have significant magnitudes only at $\phi = 0$ and at $\phi = \pm k$. The corresponding Fourier plane distribution therefore reduces to three points of light, one at the optical axis, the others displaced from the axis by distances equal to $\pm Ff\lambda$. The displaced light is reduced in amplitude by the factor $a/2$ relative to the undisplaced light. These three components evidently correspond to the mean level or 'dc' component within $A(z)$ and the sinusoidal component that has effectively modulated the mean level.

The above argument may be extended by consideration of more complicated transmission distributions $A(z)$, in which case further focused points of light will be found in the Fourier plane displaced from the axis by distances $\pm Ff\lambda$ where f now applies in turn to each spatial frequency component present within $A(z)$. The vertical axis in the Fourier plane may in fact be calibrated in terms of spatial frequency, whilst the amplitude of each focused point of light will be proportional to the magnitude of the corresponding spatial frequency component. If the transmission distribution contains components in directions other than z the direction of displacement in the Fourier plane is similarly inclined to the vertical axis. Thus the amplitude distribution within the Fourier plane is a true two-dimensional Fourier transform of the amplitude distribution of the light leaving the transparency, and is therefore related to the two-dimensional spatial frequency spectrum of the information contained within the transparency. An important factor governing this relationship will be considered in Section 3.2.

Note that a Fourier transformation of the above type takes place wherever the illumination proceeds from a point source, whether or not the source is at infinity i.e. whether or not the light incident upon the transparency is truly collimated. When the wavefronts reaching the transparency are spherical rather than plane, the imaging lens brings them to focus at a plane other than the rear focal plane as on-axis and displaced images of the source.

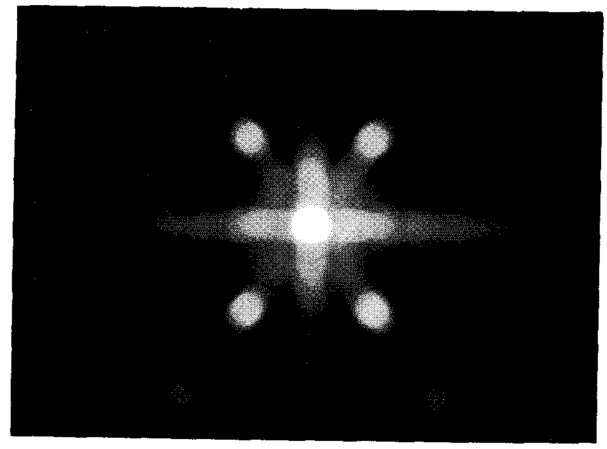

Fig. 4 - Fourier plane pattern produced when Test Card C transparency is illuminated by narrow-band light from a small pinhole

Fig. 4 is a photograph of the Fourier plane distribution obtained when the transparency was a print of Test Card C illuminated by a very small and narrow-band light source. The contrast ratio was such that the central area, corresponding to mean level and low-frequency components, had to be grossly overexposed to record the light that was further displaced, but components corresponding to the resolution bars and in particular the corner bars can be clearly discerned.

When non-collimated light is used, the expression which determines the displacement of Fourier components contains a term dependent upon the degree of divergence or convergence of the incident light. This is a useful property, because small adjustments to the spatial filtering obtained with a filter of fixed size can be made by altering the position of a collimating lens. Such adjustments do not effect the size or position of the resulting image, but the location of the spatial filter has to be altered to follow an axial movement of the Fourier plane.

2.2. Subsequent Image Formation

The light converging to focused points in the Fourier plane subsequently diverges again, its wavefronts remaining spherical. In fact the light now behaves as though the points of focus had been a set of radiating sources, rigidly locked together in frequency; and it is helpful to consider them as such.

Synchronous radiating sources of lower frequency are often used as radar and navigational aids because they produce a stationary pattern of interference. It is well known that for two such sources the interference pattern takes the form of a set of confocal hyperboloids having the two sources as their common foci. At distances from the sources sufficiently large compared with their spacing these hyperboloids approximate to a set of cones which share the mid-point of the line joining the sources as a common apex. This approach will now be applied to the propagation of light from the Fourier plane to enable an assessment of the subsequent image formation to be made.

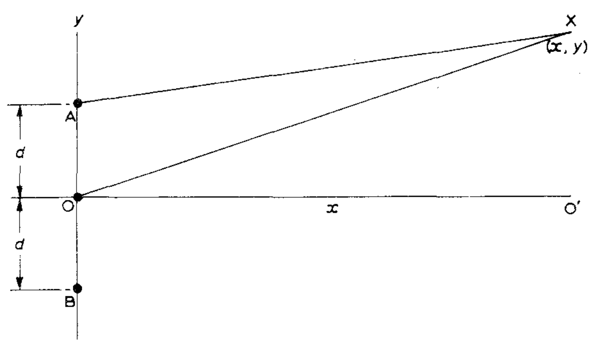

Fig. 5 - Diagram used in calculating propagation after Fourier plane

Fig. 5 shows at O and A two supposed light sources in the Fourier plane. Source O is on the optical axis OO′ and corresponds to the mean level component. Source A is displaced from O by a distance d and together with source B corresponds to a given spatial frequency component f, where $d = Ff\lambda$. O and A are radiating synchronously and have a phase difference that is expressible as a path difference $t\lambda$. Consider the amplitude produced at a point X which is at co-ordinates (x,y) with respect to O. If X is at a point where radiations from O and A reinforce, then

$$\mathrm{OX} = (\mathrm{AX} - t\lambda) + n\lambda$$

where n is an integer which could be positive or negative.

Now $\mathrm{OX}^2 = x^2 + y^2$, and $\mathrm{AX}^2 = x^2 + (y - d)^2$. Substituting from these last two equations into the first, we arrive at

$$\frac{4(y - \frac{d}{2})^2}{(n - t)^2\lambda^2} - \frac{4x^2}{d^2 - (n - t)^2\lambda^2} = 1$$

This is the equation of a set of confocal hyperbolae (each one corresponding to a particular value of n) having the points O and A as common foci. Now if $(n - t)>0$, OX>AX and therefore the y co-ordinate of X exceeds $d/2$. Hence in this case, only the upper right-hand quarter of the hyperbola is relevant. Correspondingly, if $(n - t)<0$, OX<AX and only the lower right-hand quarter is relevant. If $x>>d>>n\lambda$, the equation of the relevant half of the hypobola can be simplified to

$$y - \frac{d}{2} = x\frac{(n - t)\lambda}{d} \qquad (1)$$

This represents a pencil of straight lines passing through $(0, d/2)$, the mid-point of OA.

Now consider the sources O and B. For simplicity we assume that the transparency has an amplitude transmission factor $A(z)$ of the form $A(1 + a \cos kz)$, i.e. that there is complete symmetry about a horizontal plane containing the optical axis. Then the path difference between the radiations emitted from O and B is also $t\lambda$. The interference pattern produced by O and B can now be obtained by an argument similar to the above. The relevant half-hyperbolae in this case reduce when $x>>d>>m\lambda$ to

$$y + \frac{d}{2} = -x\frac{(m - t)\lambda}{d} \qquad (2)$$

which represents a pencil of straight lines passing through $(0, -d/2)$, m being another integer.

Now consider the points where these lines cross those due to O and A, i.e. where there is reinforcement of light from all three sources. This happens where Equations (1) and (2) apply simultaneously, i.e. where

$$x = \frac{-d^2}{(m + n - 2t)\lambda}$$

Note particularly that if we move from one of the straight lines associated with O and A to the next one by, say, increasing n by 1, and at the same time move from one of the OB lines to its neighbour by decreasing m by 1, the above expression for x remains unaltered. This means that the many crossing points obtained by exploring every combination of values of m and n are contained within a series of straight lines at right angles to the optical axis. These intersections are shown diagrammatically in Fig. 6. We shall be giving special consideration to the set defined by making $m = -n$, i.e. $x = d^2/2t\lambda$, for a reason which will become apparent when we have evaluated $t\lambda$.

To determine $t\lambda$ we make use of the principle of equal optical path[8] which states that the optical path length* between any two orthogonal surfaces

* The optical path length between two points is equal to the product of the velocity of light in vacuo and the time taken for light to travel from one point to the other.

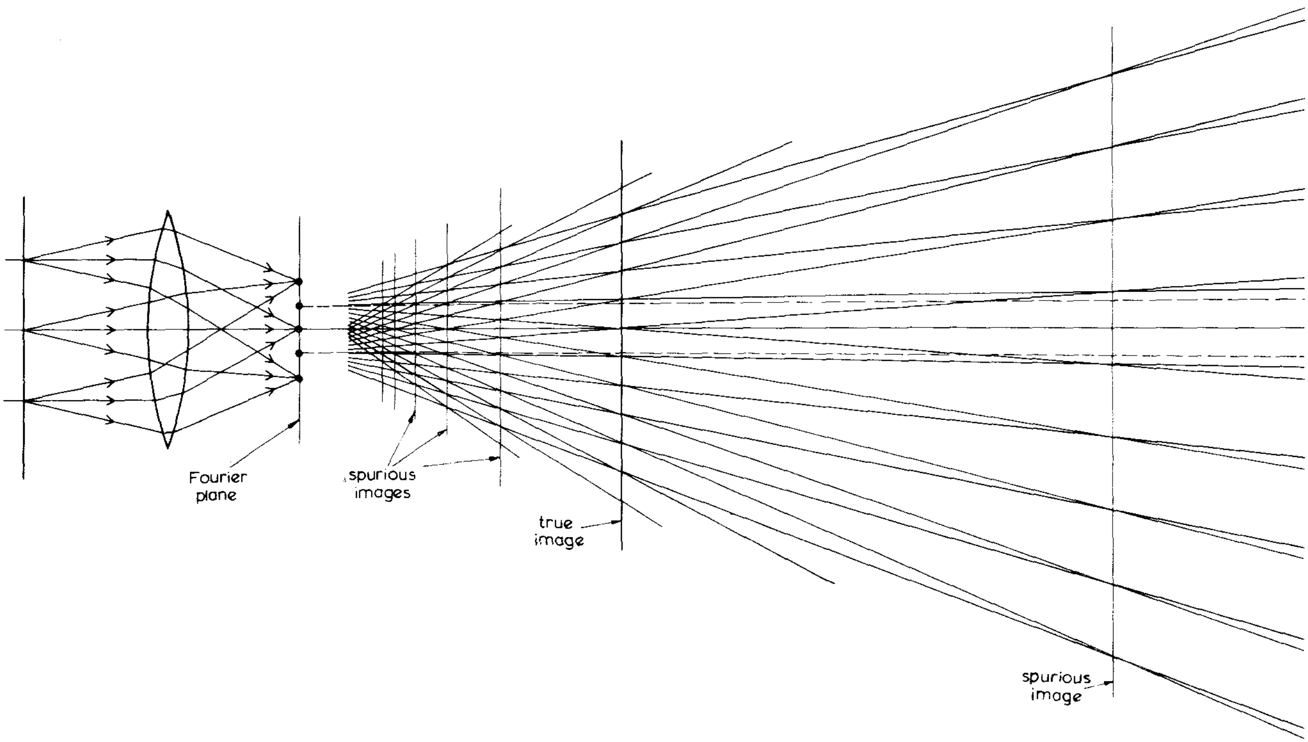

Fig. 6 - Diagram showing occurrence of spurious images

(wave fronts) is the same for all waves. Fig. 7 shows at (*a*) two rays PO and QQ′O which have passed through the transparency and are converging at O to produce an image of the source, the latter being effectively located at infinity. The line PQ, which indicates the front focal plane of the lens, can also define a typical wavefront, and the above principle therefore implies that the time taken by the ray travelling from Q through Q′ to O is equal to that taken by the ray travelling from P to O.

In Fig. 7(*b*) are shown two rays leaving the transparency at A and B respectively. One of them, APO, is repeated from Fig. 7(a). The other, BPQ′D is a deflected ray caused by the presence of a spatial frequency component on the transparency. Point B, and the particular spatial frequency component considered, are chosen in such a way that after leaving B the ray passes through P and reaches a point of displaced focus D where OD = QP. A comparison of Figs. 7(*a*) and 7(*b*) now enables us to say that the time taken for the first of this second pair of rays to travel from P to O is equal to that taken for the other to travel from P through Q′ to D. This means that the difference between the times taken by rays AO and BD is equal to the time difference that occurs between AP and BP. Thus the required path difference $t\lambda$ is given by

$$(\mathrm{BP} - \mathrm{AP}) = \mathrm{AP}(\sec\theta - 1)$$
$$= (u - F)(\sec\theta - 1)$$

But $\tan\theta = d/F = Ff\lambda/F = f\lambda \ll 1$

So that $\sec\theta = (1 + f^2\lambda^2)^{1/2} \approx 1 + \frac{1}{2}f^2\lambda^2 = 1 + d^2/(2F^2)$

Therefore $t\lambda = (u - F)d^2/(2F^2)$

Now the distance from the lens to the line joining crossing points for which $m = -n$ is given by

$$x + F = \frac{d^2}{2t\lambda} + F = \frac{F^2}{u - F} + F = \frac{uF}{u - F}$$

Therefore calling this distance $-v$, we have

$$\frac{1}{u} - \frac{1}{v} = \frac{1}{F}$$

$x = d^2/2t\lambda$ thus defines the position of the image of the transparency which the classical lens formula would lead us to expect. The above working has shown, moreover, that it is only at this position, where $m = -n$, that crossing points occur irrespective of the spatial frequency f that produced them. As Fig. 6 indicates, there are a number of spurious image positions corresponding to the crossing points for which $m \neq -n$. A different set of such images occurs, however, for each spatial frequency present, and it is only at the true image position that all of the sets coincide. An example of a spurious image is given in Fig. 8. This photograph was taken at a point where the majority of the test card is defocused, but the centre of the group of resolution bars is clearly defined.

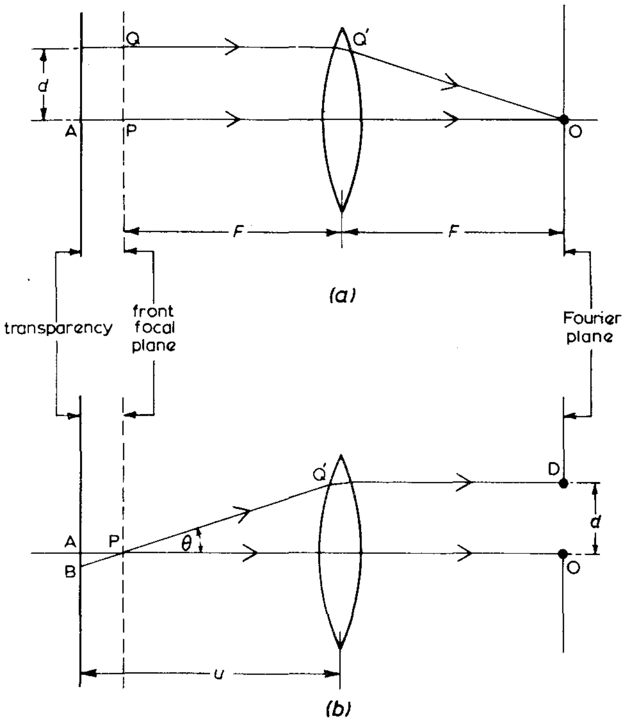

Fig. 7 - Diagram used in calculating path difference $\delta\lambda$

(*a*) showing two rays undeflected at the transparency
(*b*) showing one undeflected and one deflected ray

It is interesting to observe the way in which the image is built up in the region between the Fourier and true image planes. At the Fourier plane one sees a distribution of the type shown in Fig. 4. As one moves away from the Fourier plane the central blob is seen to expand, absorbing successively higher-frequency components in turn. As they become absorbed the various components move to take up their correct positions within the image, exhibiting a number of spurious foci of the type illustrated in Fig. 8 as they do so. Fig. 9 is a photograph taken at a point quite near to the Fourier plane. Already, however, the very-low-frequency components have moved nearly into their final positions and a low-definition test card has appeared. Higher-frequency components, notably those relating to the corner bars, have not as yet been absorbed into the image.

If now the light source is enlarged in size, the equivalent sources shown in Figs. 5 and 6 are similarly enlarged, because they are images of the original source. Each elementary point within the original source produces an associated group of image points in the Fourier plane and each such group produces a series of reinforcement loci as illustrated in Fig. 6. The loci corresponding to different source points, however only come into coincidence at the true image position. At spurious image positions the crossing points associated with different source points still lie in the same vertical plane, but they are separated from each other so that where originally there was one point there is now a spread of points. This means that as the original source is enlarged, the spurious images illustrated by Fig. 8 become less easily defined, particularly those at some distance from the true

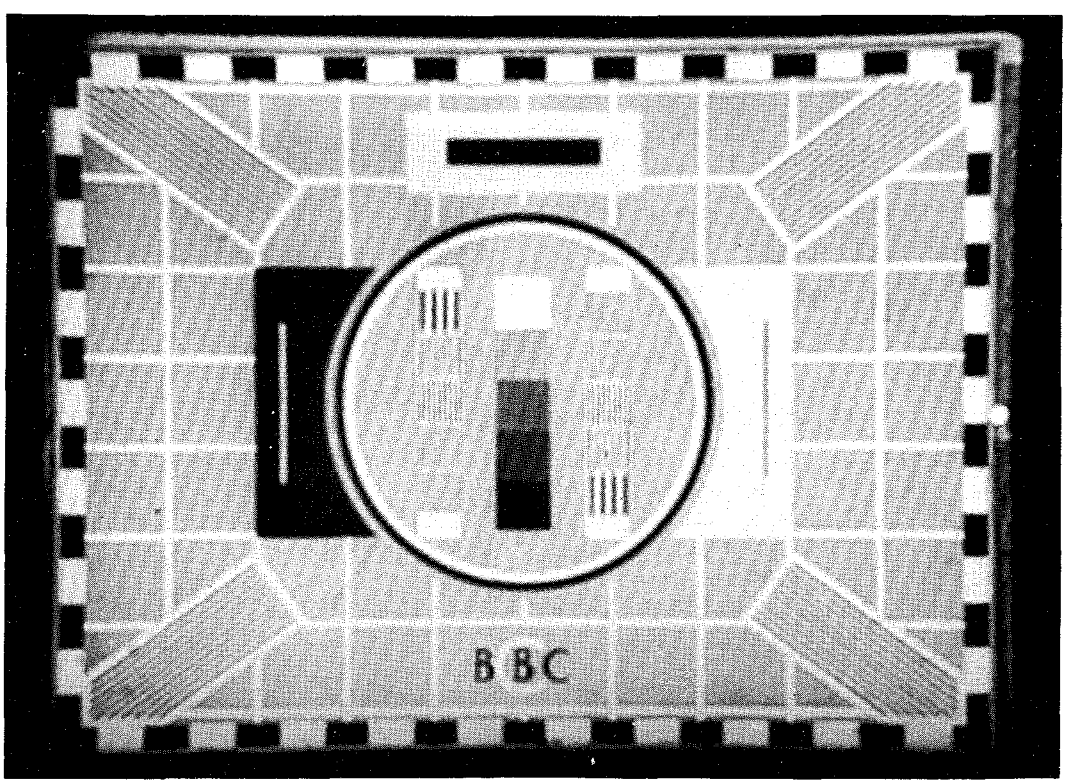

Fig. 8 - Photograph of Test Card C taken at a spurious image position

image plane. Ultimately, as the illumination of the transparency becomes completely diffuse, the modulation depth associated with spurious images becomes very low[9], and their visibility is therefore greatly reduced, if not completely eliminated.

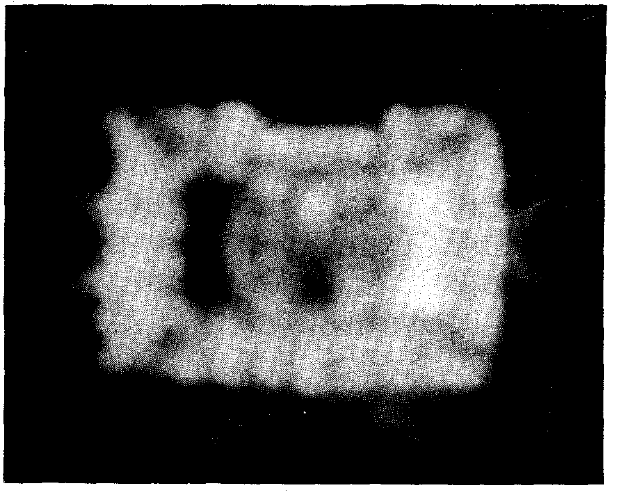

Fig. 9 - Photograph of Test Card C taken at a short distance from the Fourier plane

3. APPLICATION TO IMAGING OF FILM

3.1. Basic Optics

In order to examine the phenomena associated with spatial filtering under realistic conditions an optical arrangement was devised which it was thought might be suitable for the production of 16 mm down-printed film from 35 mm negative material. This arrangement is shown diagrammatically in Fig. 10. The source S was a 12V 100W projector lamp which produced an intense and quite well-focused beam. The pinhole P was placed at the point where the light flux from the lamp was most concentrated. A small piece of diffusing glass was attached to the pinhole on the side nearer to the lamp. This was included because with the pinhole present the system had a large depth of focus, and unless a diffuser was used a well-focused image of the filament appeared at the transparency O and was thence relayed to interfere with the wanted image at I. The pinhole was circular of diameter 0·5 mm; it was initially thought that this size, together with a modest degree of spatial filtering, would enable film exposures of about 1/100 sec to be used at I, these being durations suitable for conventional printing machines.* Lens L1 was placed so that its focal point coincided with P, and emerging from L1 was a nearly parallel beam used to illuminate the object transparency O. L1 was a 3 in. (75 mm) f/2 lens. Its diameter was thus sufficient to produce a parallel beam filling the 35 mm format, whilst its accompanying short focal length allowed it to accept a 29° cone of rays from the pinhole.

After passing through the transparency the light entered lens L2, and a Fourier plane distribution was formed at the focal plane F. L2 was a 2 in. (50 mm) f/2 lens. It is desirable (see Section 5) that the displacement from the axis at F of components corresponding to a particular spatial frequency shall be as large as possible in comparison with the size at F of the image of P. Both of these quantities are varied by altering the focal length of L2, but their ratio remains constant. In order, therefore, to increase the size of the Fourier plane distribution with respect to that of the pinhole image, one has either to decrease the size of the pinhole or to increase the focal length of L1. The ratio could be doubled, for instance, by halving the pinhole diameter or by doubling the focal length of L1. Either of these measures, however, would reduce to one quarter the illumination received at O and thus necessitate a four times greater exposure at I. We thus conclude that the above ratio may only be increased without prejudice to the required exposure if the illumination of the pinhole is increased. The implications of this result will be examined in Section 5.

The lenses used gave a pinhole image at F of diameter 1/2 mm $\times$ 2/3 = 1/3 mm. The highest spatial frequency of interest in the 35 mm transparency was about 14 c/mm, so at a mid-band wave-

* It was later found that considerably longer exposures might be necessary for the relatively insensitive film stocks used for positive printing.

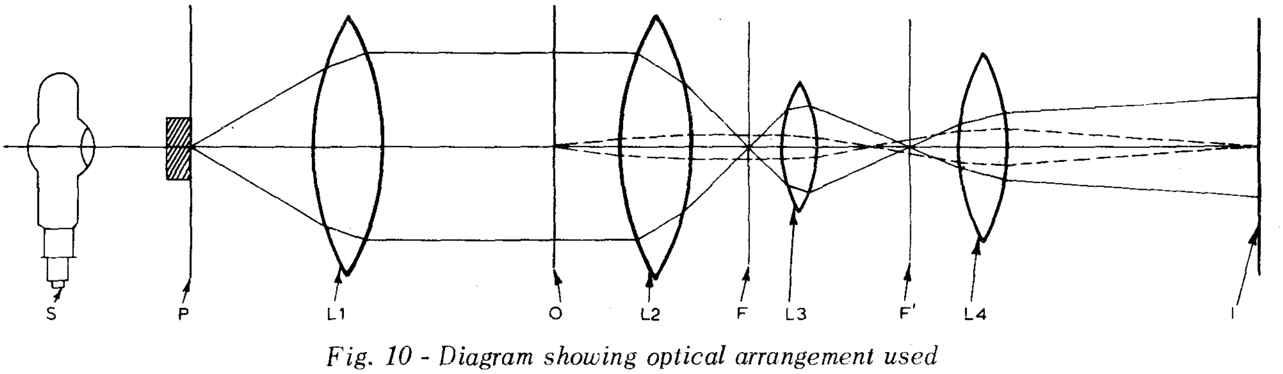

Fig. 10 - Diagram showing optical arrangement used

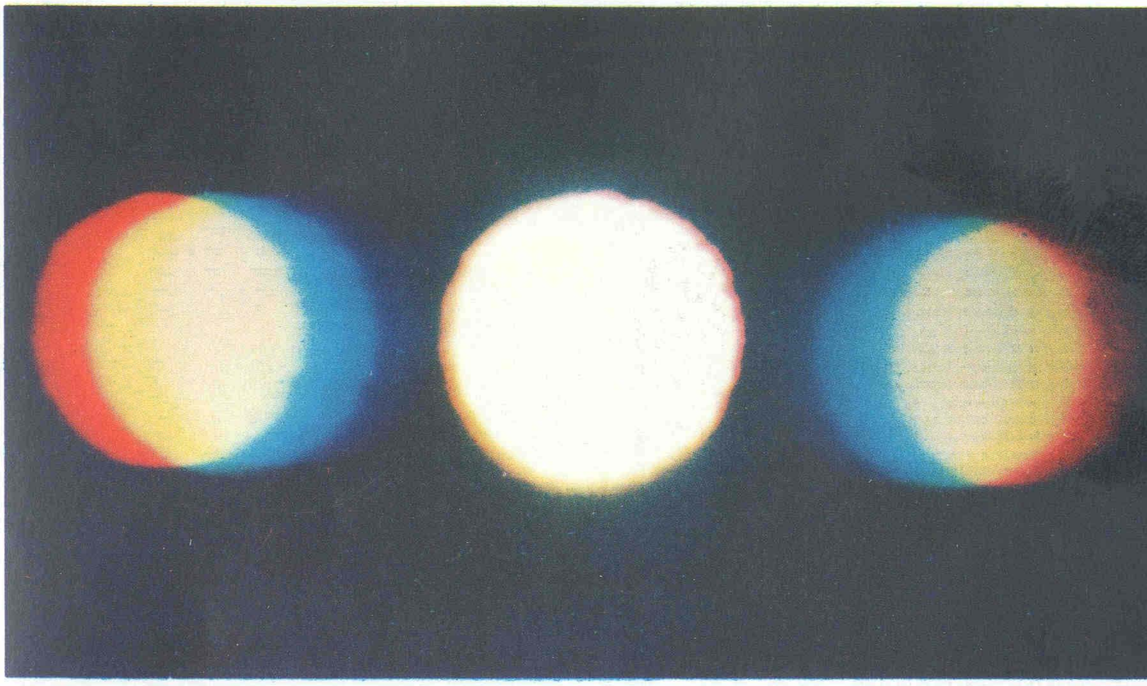

Fig. 11 - Photograph of Fourier plane when a sinusoidal grating was used as the transparency

length of, say, 560 nm, the displacement from axis occurring at F is given by

$$d = Ff\lambda$$

$$= 2.25 \cdot 4.14 . 560 . 10^{-6} \text{ mm}$$

$$= 0 \cdot 39 \text{ mm;}$$

at 390 nm and 680 nm, the approximate peak sensitivity wavelengths of the print stock blue and red sensitive layers, the corresponding values of d are 0·27 mm and 0·45 mm.

Thus, in the arrangement used, the Fourier plane displacement was not greatly in excess of the diameter of the pinhole image. Fig. 11 is a photograph of the Fourier plane distribution produced when the transparency contained a sinusoidal grating pattern of frequency somewhat in excess of 14 c/mm. As the calculation has suggested, the displaced images of the pinhole which are produced by the sinusoidal component only just separated from the axial image corresponding to the mean level component. The effect of the splitting of displaced images into their chromatic components, also evident in Fig. 11, will be discussed in Section 3.2.3.

The distribution at F, therefore (Fig. 10), had a total width of only just in excess of 1 mm. The mechanical precision necessary to do accurate filtering at F would consequently have been inconvenient for experimental purposes. If the focal length of L2 had been, say, 16 in. (406 mm) instead of 2 in. (50 mm) the Fourier pattern would have approached 10 mm across. In the absence of other lenses, however, the distance between the transparency and the image of it that L2 produced would have needed to be about 72 in. (1·8 m). In order to achieve a compact arrangement, therefore, it was decided to use a 2 in. (50 mm) lens for L2 and follow this with a 1 in. (25 mm) lens L3 which formed at F′ a suitably magnified image of the Fourier plane. Spatial filtering was carried out at F′. Meantime since O was mounted close to L2, a virtual image of O was formed on the same side of L2, but somewhat further away from it. This was then relayed by L3 to give a real image of approximately 16 mm format size close to the rear element of L3. A further lens L4, of 5 in. (127 mm) focal length, was used to relay this image, after filtering at F′, to the final image plane I. The complete arrangement was thus contained within a distance of about 30 in. (762 mm).

Fig. 12 shows the arrangement used, and also indicates the path taken by the light. The pinhole diffuser was removed whilst this photograph was taken, and the cone of rays shown leaving the pinhole is about equal to that accepted by the collimating lens L1. The photograph shows a small camera set up to record the filtered image.

3.2. Complications Encountered in Practice

It has already become apparent that the arrangement for spatial filtering investigated was in

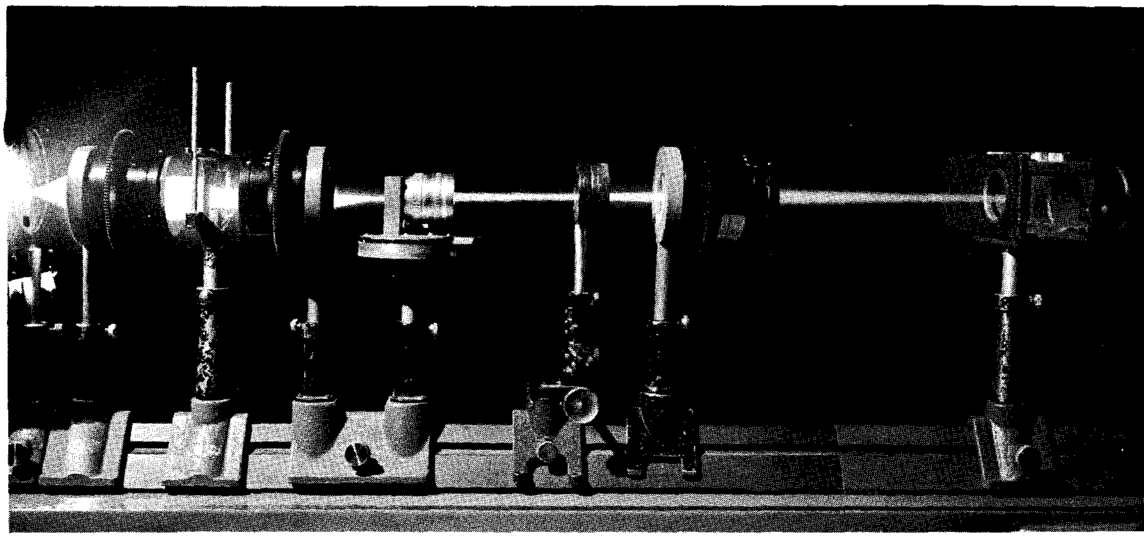

Fig. 12 - Photograph of optical arrangement

some important respects different from the idealized arrangement shown in Fig. 1. Four notable complications occurred in the practical arrangement, and these will now be examined.

3.2.1. Phase Modulation and Film Scatter

In Section 2.1 it was assumed that the negative transparency merely modulates the amplitude of the light passing through it. In fact, however, the silver or dye image present on the film has associated with it changes of refractive index and in particular a relief image at the surface. These additional properties cause the light to be modulated in phase as well as in amplitude. The degree of phase modulation can be substantial, as Fig. 13 indicates. These photographs are of the surface of two types of film stock, taken with the aid of an interference microscope. They show the interference produced between reflections of nearly monochromatic light from the surface of the film and from an optically flat glass plate placed just above the film plane and very slightly inclined relative to it. Thus a movement from one of the fringes to its neighbour implies a change in the distance between the film surface and the reference plate of half a wavelength. Fig. 13(*a*) shows the surface of a black-and-white test card print in the region of the lowest frequency resolution bars. The relief image of the bars has a height of half a wavelength. This means that light travelling through the thickest part of the image has to traverse an extra half wavelength immersed in a medium of refractive index, say, 1·5, whilst light travelling through the thinnest parts covers the same distance in air of refractive index nearly unity. The former light therefore becomes retarded in phase with respect to the latter by about 90 degrees.

Fig. 13(*b*) shows the corresponding relief image associated with the highest-frequency bars. Fig. 13(*c*) shows the relief image associated with a black-to-white transition on a colour negative. One of these fringes has been inked in to facilitate identification, and it can be seen that this relief image has a height of about a wavelength, after the disturbance in the region of the transition has settled down.

If a perfect lens is used to form an image of the transparency, and there is no spatial filtering, this phase modulation is merely transferred from the object to the image plane, at which it is disregarded by the film as the latter records the intensity pattern only. At only a short distance from the image plane, however, the phase modulation produces a spurious amplitude modulation. This is illustrated in Fig. 14 which shows three images of a test card which was bleached over half its surface and illuminated by well-collimated light, one taken at the true image position, the others at positions on either side of and just displaced from the true image. The bleaching enables the effects of phase modulation to be observed in isolation. The height of the relief image was in fact enhanced by the bleaching process, and it may therefore be that the phase-modulation effects are not evident at positions quite so close to the true image as these photopraphs would suggest; nevertheless it is believed that quite critical focusing is needed to avoid them.

The formation of these spurious images may be simply described by Fig. 15. This shows at (*a*) a series of parallel rays travelling through a negative transparency in the region of a change in thickness produced by a relief image. As they leave the transparency the rays that encounter the edge of the transition are bent away from their original parallel paths. The transition behaves in fact similarly to a concave followed by a convex lens. The corresponding ray pattern at the image is shown in Fig.

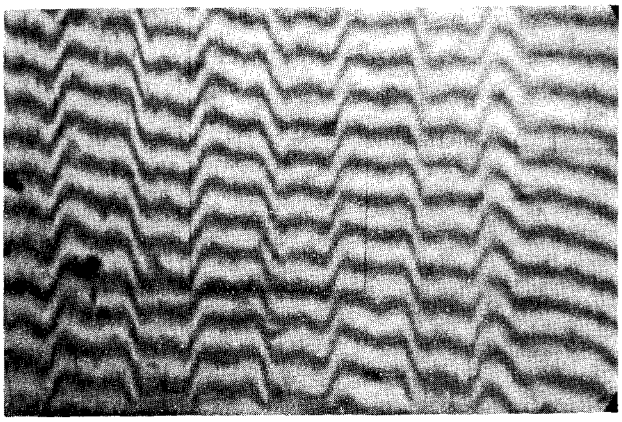

(a)

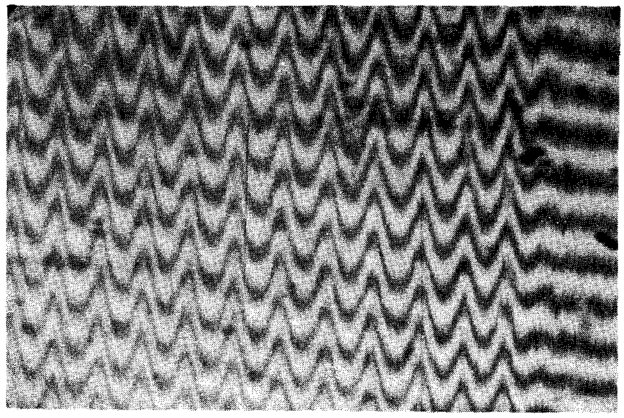

(b)

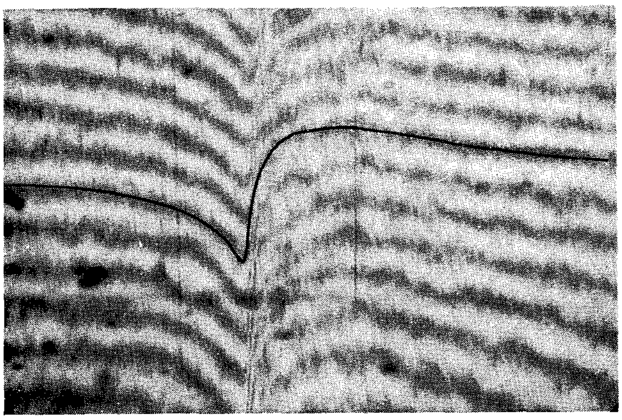

(c)

Fig. 13 - Photographs of surface of film taken using interference microscope

(*a*) Lowest frequency resolution bars on 35 mm black-and-white Test Card C print.
(*b*) Highest frequency resolution bars on above print.
(*c*) Black-to-white transition on colour negative

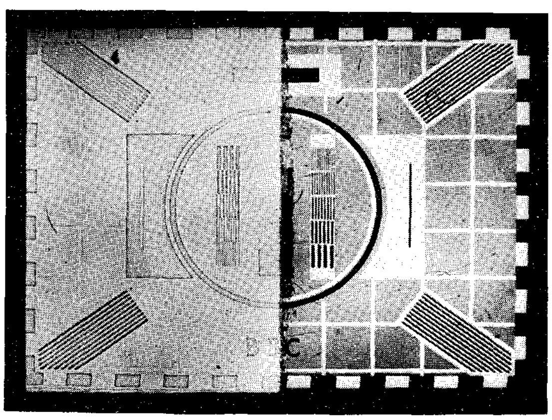

(a)

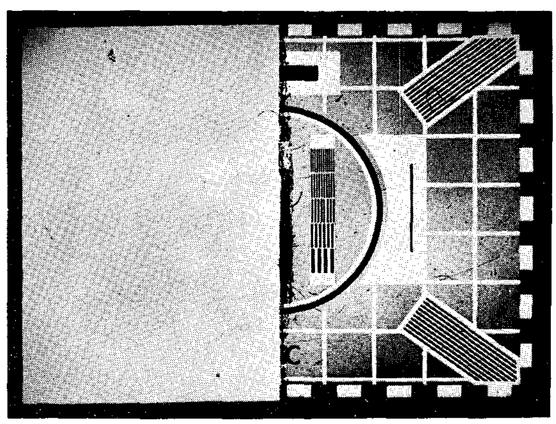

(b)

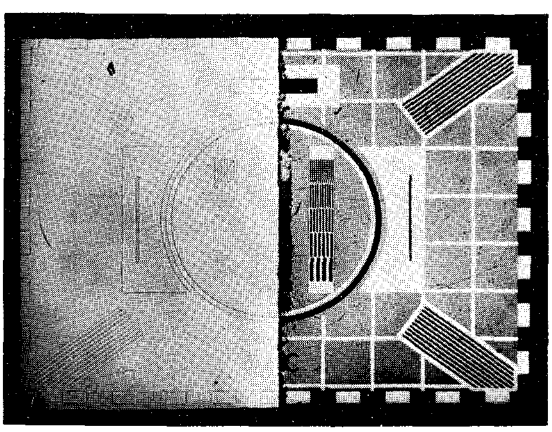

(c)

Fig. 14 - Photographs of half-bleached Test Card C taken

(*a*) at point slightly to one side of true image position
(*b*) at true image position
(*c*) at point slightly to the other side of true image position

15(b). Assuming that there are no aberrations in the system this pattern is similar to that at the object, with the exception that there is here no refracting surface to make the rays parallel again. At I the illumination is virtually even, and no image appears. At L and M, however, the bunching of rays produces an uneven intensity distribution characterised by a reduced illumination on one side of the transition and an enhanced illumination on the other side. If the transition profile is skew-symmetrical about its mid-point, the distribution obtained at M is the reverse of that at L. These properties can be recognised in Fig. 14, which shows also a granularity introduced at what were areas of high density by the remains of a grain relief structure.

Meantime the distribution obtained in the Fourier plane represents a spectrum corresponding to both amplitude and phase modulation. If any spatial filtering is carried out, some of the phase modulation is converted to amplitude modulation, and thus displayed as a spurious image component at the true image plane.

This suggests, as does Fig. 14, that it may be possible to obtain some improvement in the resolution of fine detail by making use of the phase modulation effects. They are in fact quite likely to have some influence on the final image if well-collimated illumination is used, unless care is taken to avoid their occurrence or to prevent a subsequent conversion to amplitude modulation. The sometimes beneficial influence of the relief image has been noted by workers in optical printing[10]. The contour of the relief image does not exactly correspond, however, to the image produced by absorption (see for example Fig. 13(b)), and it cannot necessarily be used, therefore, to provide equalisation of the required form. The mode of conversion to amplitude modulation too would not necessarily have the required characteristics. It is doubtful, for example, whether a spurious image of the type illustrated in Fig. 14 would if added to an uncorrected image improve its appearance. Moreover the phase modulation might show considerable variations from one film stock to another, if not between different batches of the same stock.

In any case, Fig. 14 also illustrates a related and very undesirable effect produced by the specular illumination of film – the increased visibility of the images of scratches and other surface blemishes. Such defects could be considered as producing an extreme amount of phase modulation, some of the spectral components being so deflected that they are no longer intercepted by the imaging lens. This enhancement of surface defects can seriously mar the appearance of the print and it is therefore not unusual to immerse the film in a suitable liquid during printing[11]. The liquid fills up the scratches, and evens out the surface so that all of the effects described above are substantially removed. It is therefore considered that liquid printing should continue to be used in the presence of spatial filtering, the latter being designed to achieve the optical equalisation required without the complications that phase modulation effects would have introduced.

There remains the possibility that some light would be randomly deflected by scatter within the film. This would produce an image component formed as by diffuse illumination, the corresponding rear focal plane distribution being random. It is not expected, however, that the consequently unfiltered image contributed by this scattered light would have an intensity sufficient to prevent the required optical correction from being applied.

3.2.2. Gamma

The negative is usually processed to a gamma of about –0·6.

This statement of gamma implies a measurement of the attenuation of light passed through the film. All practical light sensitive devices respond to the intensity (given by the square of the amplitude) of the incident light; the Fourier plane, however, represents the transform of the amplitude distribution at the transparency. Therefore filtering at the Fourier plane effectively operates upon the imaged scene at a gamma not of –0·6 but of –0·3.

Now an inspection of Fig. 2 together with the corresponding curve obtained by measurement of the 35 mm negative stock shows that it is in the production of the 16 mm down-print that the majority of the loss of resolution occurs. It seems reasonable to suppose, moreover, that it comes about during the formation of the latent image within the positive stock emulsion, i.e. at a gamma of –0·6.

The implication of this is that if spatial filtering is used, correction is made to a signal given by the square root of the signal whose distortion it is desired to compensate.

To ascertain how serious is this limitation a simple experiment was conducted using a flying-spot slide scanner. It was possible to use this as an analogue to the film process because it contained both high-pass equalisation and gamma-correction circuits. In its normal operation, the high-frequency content of the signal was first boosted in an aperture corrector by up to 10 dB in order to offset the loss caused by the finite size of the scanning spot, and the gamma was then lowered to about 0·45 to compensate for the gamma of the final display tube. The experiment consisted of using two signal processing chains in parallel, one standard and the other modified by interchanging the circuits so that aperture correction was taking place at a gamma of

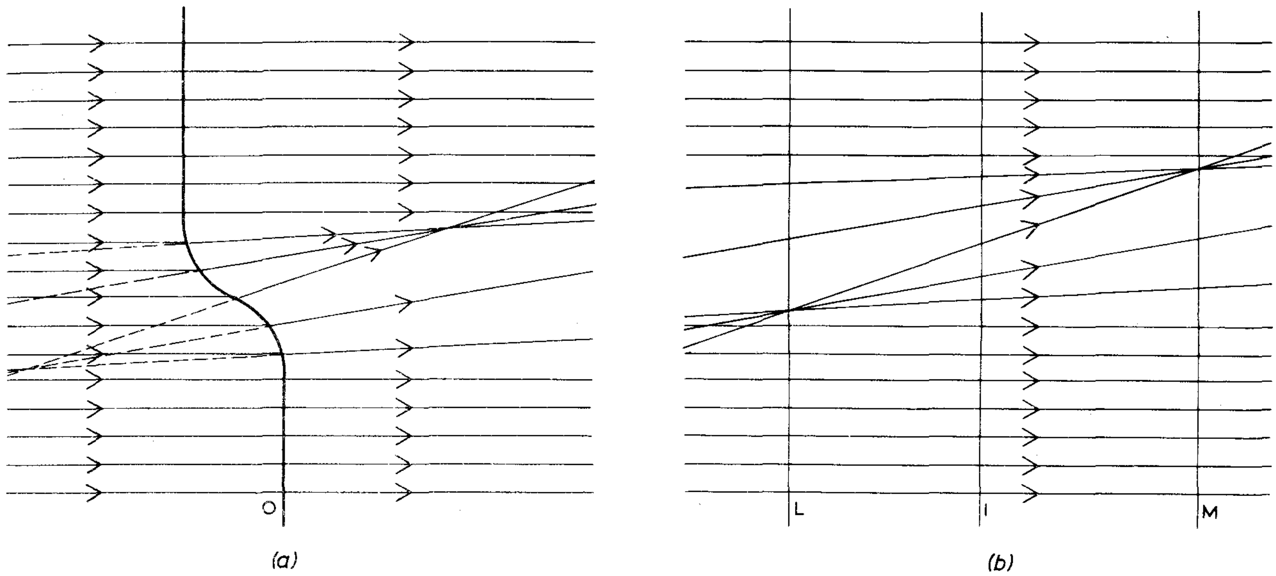

Fig. 15 - Diagram showing rays associated with relief image

(*a*) at transparency (*b*) at image

0·45 instead of unity, and arranging to switch the two outputs in turn to a picture monitor. When an SMPTE test card slide was used the modified signal chain was found to produce a small increase in the mean level associated with the highest frequency resolution bars. Apart from this however, and for a range of pictures of normal scenes, no difference between the two outputs could be detected. Indeed, a method of 'level–dependent aperture correction' which is in some respects similar to aperture correction after gamma correction is becoming usual in the design of colour television camera signal processing circuits because of its benefit to noise performance. It appears, therefore, that an impairment to the spatial frequency spectrum of the image incurred at a gamma of –0·6 can be quite adequately compensated at a point in the chain where the gamma is effectively –0·3.

3.2.3. Colour Separation

As Section 3.1 has explained, and Fig. 11 has depicted, the displacement of spatial frequency components in the Fourier plane is dependent upon the wavelength of the light, and therefore the greater the spatial frequency of a given component the more the corresponding images of the source are separated into their coloured constituents.

The consequence of this is that unless the filter used in the Fourier plane is coloured, its transmission/spatial frequency characteristic will vary with the wavelength of the light. If for example the filter is neutral in colour and has a transmission which increases with radius, the red constituent of the resulting image has its high-frequency components boosted by an amount greater than that relating to the blue constituent. Now it can be argued that this is a desirable feature, because the red-sensitive layer of the print stock is underneath the other two layers, and therefore the image that it receives suffers more than do the others from diffusion within the material. As Fig. 11 suggests, however, if the separation of coloured constituents is not great as compared with the size of the pinhole image, the differences in the filter characteristics relating to different colours are small. They are greatest, of course, at the highest spatial frequencies, but the visibility of the resulting colour change at such frequencies is likely to be low, particularly in the presence of mean level and low-frequency components whose colour is not altered. Therefore although colour changes would undoubtedly be introduced by the colour separation phenomenon it is unlikely that they would prove troublesome in an arrangement of the type envisaged, in fact the small effect which they will produce could well be beneficial.

3.2.4. Finite Size of Source

Reference has already been made to the fact that the pinhole used in the experiments formed a Fourier-plane image whose size was comparable with the displacements produced by spatial frequency components present in the transparency. Indeed, for spatial frequencies much less than that used to form the Fourier plane distribution shown in Fig. 11, the displaced and axial images of the pinhole overlap. An interesting illustration of this is

given in Fig. 16. This is a record of the intensity distribution measured along a line through the centre of the Fourier plane and at right angles to a rectangular grating pattern used as a transparency. It may be seen that the axial image of the pinhole, which extends from C to K has added to it displaced images produced by the fundamental component and extending between A to H and E to M, together with much smaller images further displaced and caused by the higher harmonics. There is a degree of tilt present; this was produced because the illumination of the pinhole was somewhat uneven.

The relative magnitudes of steps AB, CD, EF, etc. are of some interest. Imagine for simplicity that the grating is sinusoidal, i.e. that the only components present are an on-axis image corresponding to the mean level component and having an amplitude a, and two displaced images of amplitude b corresponding to the fundamental component. Then supposing the transparency to be mounted at the front focal plane of the lens, so that $t\lambda = 0$ (see Section 2.2), if the light were coherent over the pinhole the three amplitude distributions would simply add where they overlapped, and the steps in the resulting intensity distribution would be given by:

$$\mathrm{AB} = b^2$$

$$\mathrm{CD} = (b + a)^2 - b^2 \qquad = a(a + 2b)$$

$$\mathrm{EF} = (2b + a)^2 - (b + a)^2 = b^2 + (2b^2 + 2ab)$$

i.e. step EF would be much greater than step AB.

If on the other hand there were complete incoherence between every possible pair of points within the pinhole, there would be a completely random phase distribution across each of the three pinhole images and therefore between one image and the others *at the places where they overlapped.* The resulting intensity distribution would then be obtained by adding the three individual intensity distributions, and the above steps would become:

$$\mathrm{AB} = b^2$$

$$\mathrm{CD} = a^2$$

$$\mathrm{EF} = b^2$$

Thus AB = EF.

The presence of other harmonic components would somewhat alter the first of these calculated relationships but would leave the second result (AB = EF) unchanged. As Fig. 15 suggests, and measurements made using several other grating patterns confirmed, it was this second relationship that was satisfied. Thus as one might have expected from the presence of the glass diffuser behind the pinhole, the light radiated from each point within the pinhole is randomly phased with respect to that radiated from the other points.

An important consideration follows from this result. Section 2.2 has suggested that the properties of a spatial filtering arrangement which uses a finite sized source of light may be determined by examining the propagation from each of a large number of sufficiently small points of light considered to comprise the finite source in turn. The light from each of these elementary sources passes through the transparency and is focused to form an associated group of points of light in the Fourier plane. One may draw in the Fourier plane a set of axes centred on the undeflected image of the elementary source and indicating where the various spatial frequency components are positioned. These axes will need to be moved about, however, as one transfers attention from one source point to another.

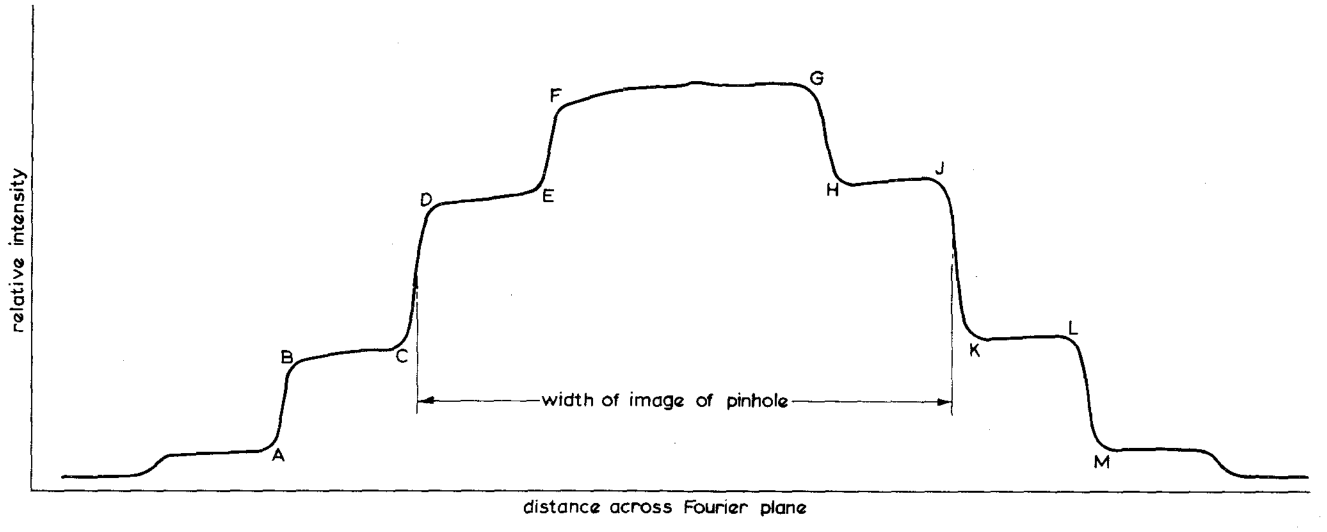

Fig. 16 - Measured distribution of intensity at Fourier plane when transparency was a square-wave grating

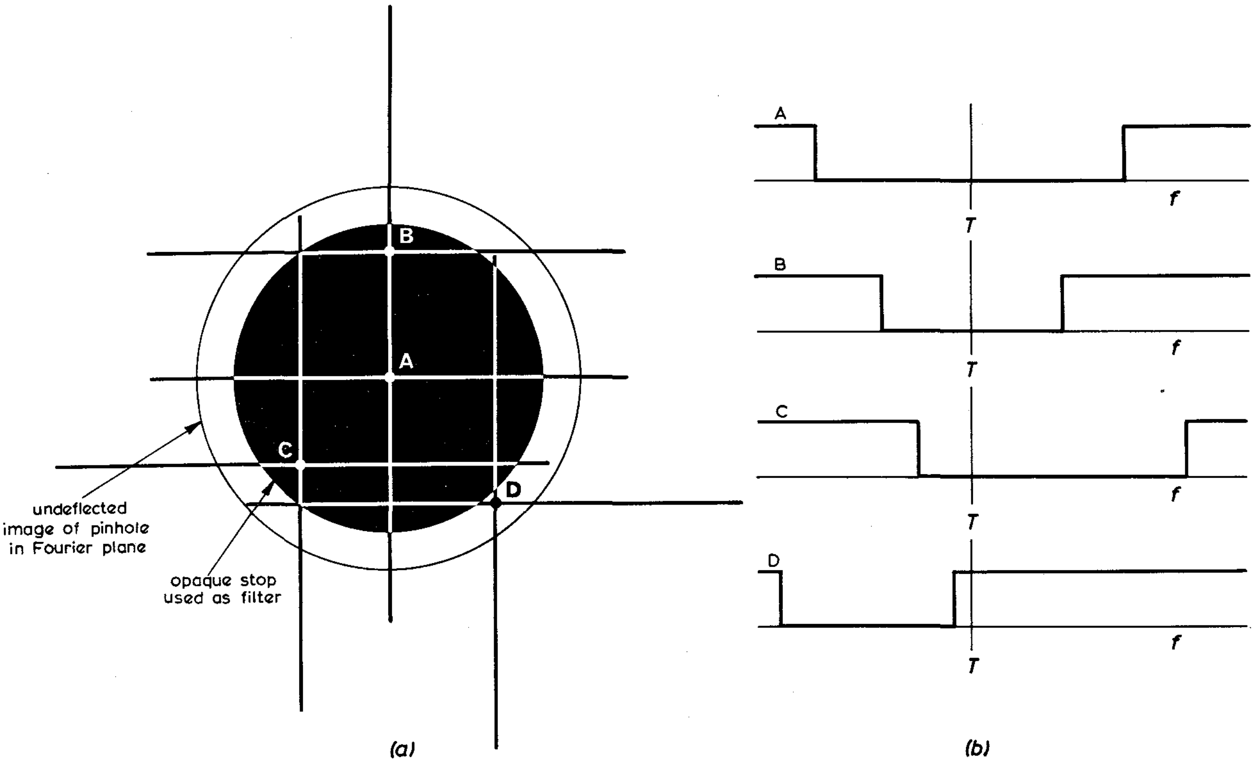

Fig. 17 - Diagram explaining multiple filtering

(*a*) showing location of images of four elementary source points

(*b*) showing corresponding transmission/frequency curves for horizontal information

Therefore a fixed spatial filter acts differently upon the information carried by the light originating from different source points. This is illustrated in Fig. 17. A, B, C and D are four points within the undeflected image of the pinhole at the Fourier plane. The axes drawn through them could have been calibrated in terms of spatial frequency and would then show the positions of the points of light associated with A, B, C and D that would occur when given spatial frequency components were present on the transparency. An opaque stop is supposed, for simplicity, to be used as a spatial filter. Its position is indicated by the black disk. The location of this disk with respect to each of the axes in turn then determines the characteristic which the filter has with respect to the information associated with points A, B, C and D. If attention is restricted to horizontal information, the corresponding transmission characteristics are as shown on the right hand side of the diagram. Only for points lying on line AB are they symmetrical, and for certain points, e.g. D, there is a low-pass component present.

Therefore when the source is of finite size, a given spatial filter acts effectively as a very large number of different filters operating in parallel. Each one produces at the image plane a filtered version of the amplitude distribution at the transparency. Since, however, the original source points are incoherently related to each other, the resulting amplitude distributions are also randomly phased with respect to each other. The resulting overall intensity distribution is therefore obtained by adding the individual intensity distributions, these being given by the squares of the individual amplitude distributions. The complete arrangement is depicted in Fig. 18, here drawn as the block diagram of an equivalent electrical circuit.

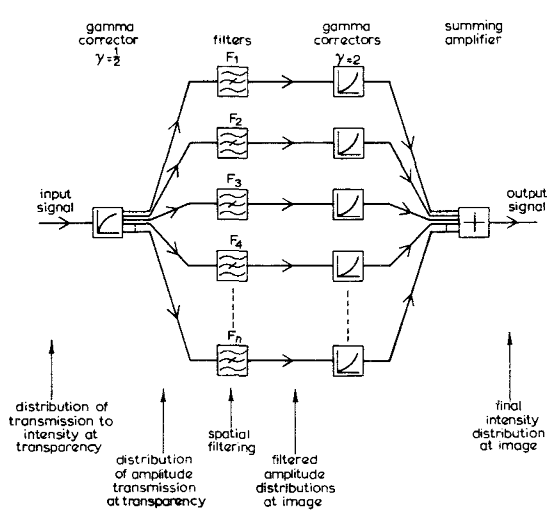

Fig. 18 - Block diagram of circuit equivalent to multiple filtering process

Thus even the simplest of spatial filters can have a very complicated characteristic when used in conjunction with a finite sized incoherent light source. The complexity increases as the dimensions of the pinhole image are increased relative to the displacements produced by information on the transparency, because there is then a greater variety of individual characteristics of the type illustrated in Fig. 17. The determination of a form of spatial filter that will enable a required overall characteristic to be achieved thus becomes a major problem. A method whereby the overall performance of specific filters may be assessed is outlined in Section 4.

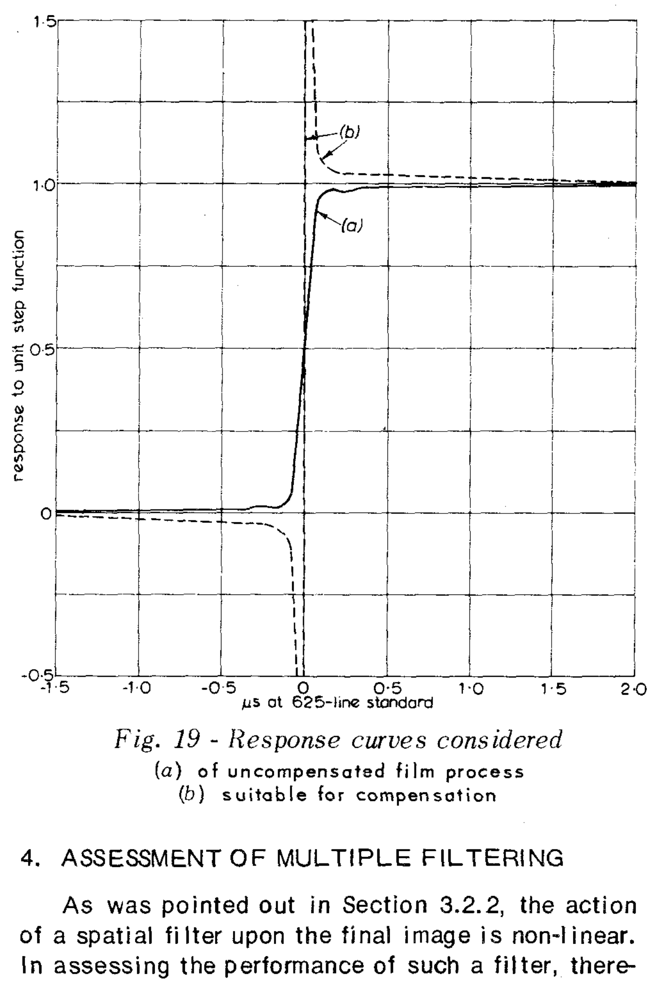

Fig. 19 - Response curves considered
(a) of uncompensated film process
(b) suitable for compensation

4. ASSESSMENT OF MULTIPLE FILTERING

As was pointed out in Section 3.2.2, the action of a spatial filter upon the final image is non-linear. In assessing the performance of such a filter, therefore, little meaning can be attached to the concept of 'frequency response'. It is however helpful to consider how a particular form of image intensity distribution is modified when the filter is present.

In judging the resolution achieved by a process of image reproduction one pays particular attention to the sharpness of outlines in the picture – the boundaries which divide areas of fairly constant luminance from each other. It was therefore thought instructive to assess the properties of spatial filters by determining the effect which they would have upon a black-to-white transition in the scene.

If such a transition is filtered in the manner indicated in Fig. 2, it becomes modified as shown in Fig. 19(a). Our aim, then, is to find a form of spatial filter which applied in the manner suggested in Fig. 18 to the distribution defined in Fig. 19(a) will produce a good approximation to a step function distribution. Alternatively, and remembering that the majority of the degradation introduced by the film occurs after the point at which spatial filtering is envisaged, we may say that if presented with a step function distribution the filter should produce a distribution whose form is similar to that shown in Fig. 19(b).

Now one particular aspect of the non-linearity involved in the process prevents the realisation of such a distribution. The output of the spatial filter, as seen by the film, is an intensity distribution. It can never, therefore, be made negative, as the left hand side of Fig. 19(b) suggests it should. A negative-going excursion introduced before a *grey*-to-white transition is both possible and desirable. When black-to-white transitions are concerned, however, any modification to the intensity distribution before the transition can only do harm. In this respect it is fortunate that the $\gamma = 2$ modification (see Fig. 18) after filtering diminishes the relative magnitude of changes introduced at the 'black' side of such transitions.

This section will investigate the performance of only one type of spatial filter, the opaque disk axially mounted. It is believed, however, that the method can be adapted for the consideration of a variety of other forms, and work is in hand to do this.

4.1. Theoretical Method

The method used to calculate the effect of filtering a black-to-white transition by means of an opaque stop followed closely the qualitative description given in Section 3.2.4. A set of elementary point sources was chosen from within the finite source, and the filtering characteristic, of the form shown in Fig. 17, was worked out for each one. The amplitude distribution at the image resulting from each of the separate filtering operations applied to the black-to-white transition was calculated. The method of calculation is described in the Appendix. The resulting distributions were then squared and added, as suggested by Fig. 18, to give the overall intensity distribution. The calculation was facilitated by the use of an electronic computer.

This method presupposes that the action of the filter upon information carried by the light originating from a given source point can be taken to represent fairly the result obtained when the whole of a certain small area of source around the point is considered. Clearly the greater the number of points used to represent the complete source the more accurate is the final result.*

* This statement assumes, of course, that in increasing the number of source points considered one does not increase the likelihood of coherence between neighbouring points.

Inspection of Fig. 17 reveals that if one divides the source into four quadrants by drawing horizontal and vertical lines through its centre, then for each point selected from one quadrant, points in each of the other three quadrants can be found for which a similar filtering action applies. A representative set of elementary sources may therefore be chosen from one quadrant only.

It was first necessary to determine how many elementary sources would need to be considered to enable the performance of the complete source to be accurately assessed. The first calculation was therefore performed four times, using 6, 22, 37 and 48 points selected from each quadrant. The locations of these points are indicated in Fig. 20 which also shows the sizes of the undeflected pinhole image and of the filter.

It was suggested in Section 3.2.4 that one may predict the position at which various spatial frequency components will cause images of a given point source to occur in the Fourier plane by imagining a set of axes centred on the undeflected image of the source and calibrated in terms not of displacement d but of the corresponding spatial frequency f, where $d = Ff\lambda$. It is now convenient to use such a calibration in quoting the dimensions of objects in the Fourier plane. Thus the arrangement depicted in Fig. 20 has an opaque circular filter of radius 2·25 MHz concentric with the undeflected pinhole image which has a radius of 2·75 MHz.

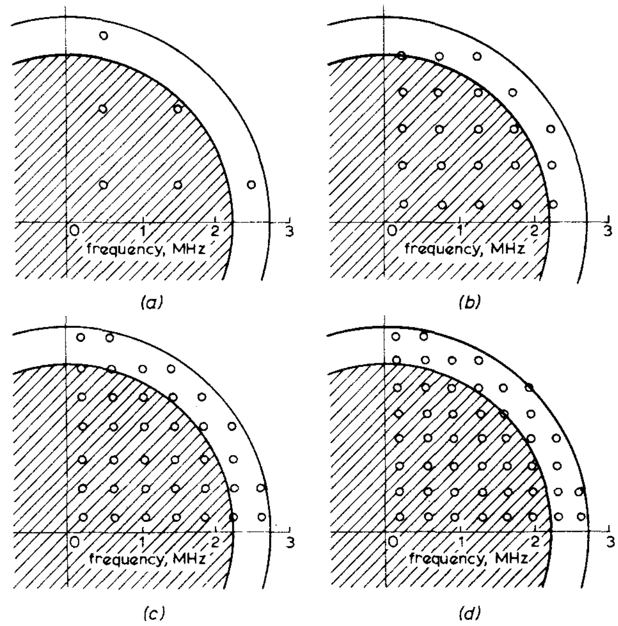

Fig. 20 - Diagram showing location of elementary source points used in first calculation
(a) 6 points (b) 22 points (c) 37 points (d) 48 points

The results of these four calculations are given in Fig. 21. They suggest that more than 6 points per quadrant are necessary but that fairly accurate results can be obtained from either 22, 37 or 48 points. It was decided, however, to continue to use

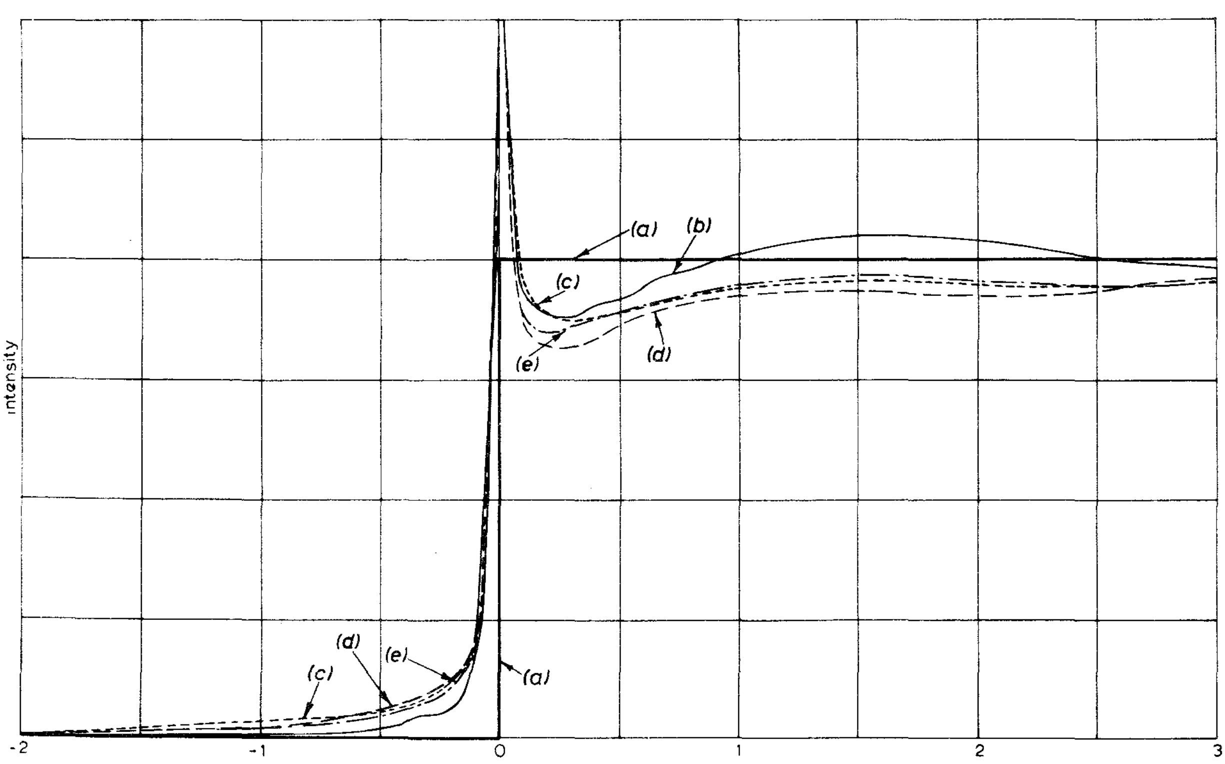

Fig. 21 - Calculated reproduction of black-to-white transition (a) using opaque stop as filter. Calculations assume:
(b) 6 elementary source points (c) 22 points (d) 37 points (e) 48 points

48 points, because the computer programme was able to handle up to 48 without using excessive time.

The calculation did not establish with accuracy the peak intensity reached at the point of transition. This value would in any case need to be modified to take into account the high-frequency limit (here assumed to be infinite) of a practical system. Nevertheless a comparison with Fig. 19 indicates that the effect of this filter is not what is desired.

In considering the resulting intensity distribution to be the combined effect of a very large number of simple filters acting independently, it should be remembered that each of these filters has abrupt transitions in its response/frequency characteristic, and thus, as the Appendix shows, when operating upon an amplitude step function it produces ringing on each side. The resulting amplitude distributions have rings of different frequencies, and if they were merely added together some degree of mutual cancellation could be expected. As explained above, however, they must be converted to intensity distributions before addition, and no such cancellation can therefore take place. This explains the slow rise in image intensity observed before the transition is reached. There are two other main characteristics. The first is a large but short-lived overshoot at the point of transition. The second is a long subsequent undershoot. The first effect is desirable; it would certainly enhance the visibility of fine detail and emphasise the outlines of the picture, giving some degree of compensation for the loss occurring later within the film process. The undershoot, however, when taken with the slow rise in level before the transition, gives the effect of a superimposed low-frequency filtering. It is produced by points such as point D of Fig. 17.

The other calculations relating to the opaque stop were made to see whether by adjusting its size relative to that of the pinhole image the edge enhancement could be improved and the accompanying low-frequency smear diminished. Stop sizes of 0·75, 1·0, 1·25, 1·5, 2·0 and 2·5 MHz radius were therefore investigated. The general form of the resulting intensity distribution was not very much altered by such changes, however. The low-frequency smear could only be significantly reduced if the stop were made so small that very little edge enhancement remained.

A particular case of interest was that for which the stop had a radius (2·75 MHz) equal to that of the pinhole image, because this excluded points such as point D of Fig. 17. The distribution resulting from this condition is shown in Fig. 22. As expected, the mean level component has now been removed, and a symmetrical form remains. The discontinuity at the point of transition becomes a

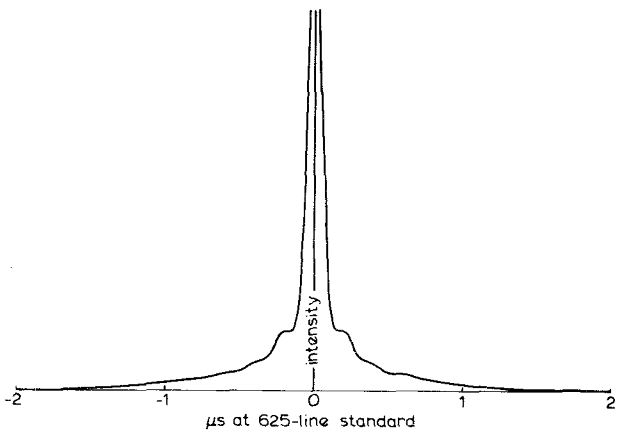

Fig. 22 - Calculated reproduction of black-to-white transition when opaque stop just removed mean-level component

narrow crevasse when the overall bandwidth of the system is restricted; the production of a well-defined dip of this type has been proposed as an aid to metrology[12].

4.2. Practical Method

The filtering action of the opaque stop upon a black-to-white transition was measured by mounting the apparatus on a lens testing bench. The arrangement of components was as shown in Figs. 10 and 12. A razor edge was mounted vertically in the object plane to act as a sharp transition. The filter consisted of a small metal disk suspended at the centre of a large aperture by means of fine wires. Its size was chosen to reproduce approximately the conditions assumed when making the first of the calculations described in Section 4.1.

In place of the camera, the bench cross slide was positioned at the image plane. It supported a fine vertical slit which was made to traverse the image in the horizontal direction. The light passing through the slit was measured by means of a photomultiplier whose output was connected to a pen recorder.

The recorded image intensity distribution is shown in Fig. 23. An approximate time scale is added so that this trace may be compared with the best theoretical curve, curve (*e*) of Fig. 21. It will be seen that good agreement has been achieved, except in one important respect. The excessive intensity recorded well to the left of the transition remained at that level when the filter was removed. It was therefore considered to be due to a veiling glare caused by scatter at the lens surfaces. Such effects are of course exaggerated when spatial filtering is used, because the sensitivity of the measuring equipment or the exposure of the film has to be increased to offset the lower photometric brightness at the image.

A black-and-white down-print made using the above arrangement proved to have the characteristics predicted above. Fine detail and edges were certainly enhanced, but the effect was marred by the smear introduced by low-pass filtering components and by a loss of contrast range caused by veiling glare. In view of these defects a print obtained without such filtering was considered to be more acceptable.

5. DISCUSSION

The foregoing has clearly established the inadequacy of the simple axial stop as a spatial filter for down-printing. This is partly due to the fact that it produces abrupt changes in the elementary filter characteristics (Fig. 17) and partly because points such as point D of Fig. 17 have associated with them a predominantly low-pass characteristic.

It is possible that some degree of useful improvement could be made to the image if two sources were used, one having associated with it an opaque stop made to remove completely the mean level component, the other being displaced from the first and having no associated filtering. This would be equivalent to adding to the unfiltered image an outline image or 'line drawing' which would emphasise edges. The amount of such correction would be limited, however, by the appearance of flare which the opaque stop also introduces, and the overall bandwidth would need to be kept high to prevent a double outline from being produced.

It is anticipated, however, that a filter whose transmission profile does not have discontinuous changes will give a much better result. Such a filter has been made by evaporating aluminium through two small holes in line onto a glass substrate. Its amplitude transmission, measured along a line through its centre, rises almost linearly from the central minimum to almost 100%. This was mounted, as Fig. 24 shows, in a liquid cell whose function was to protect it from dirt and damage and to reduce phase changes to a minimum. Being of a shiny material, however, this filter, whilst apparently effecting a worthwhile improvement to the image, introduced spurious images by multiple reflection. It appears therefore that a filter of this type would need to be elongated in one direction and then mounted in a plane which is angled with respect to the optical axis so that reflected light is no longer troublesome.

The computer programme may easily be modified so as to calculate the performance of a filter of the above triangular transmission characteristic, and this is being done. The agreement already obtained between calculation and measurement suggests that a meaningful assessment of a variety of types of filter can be made using the method outlined in Section 4.1 without the necessity for accurate manufacture and measurement.

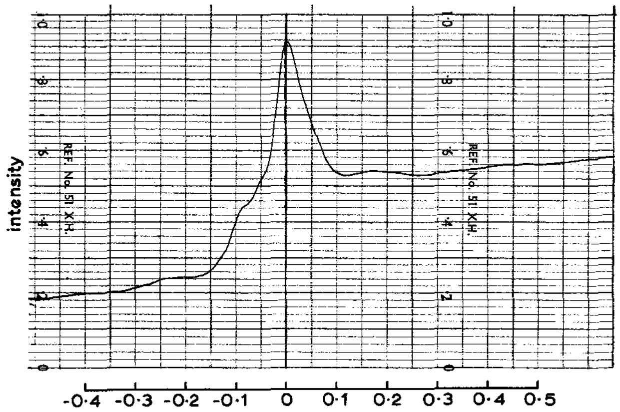

Fig. 23 - Measured reproduction of black-to-white transition when experimental arrangement was set to conditions assumed when calculating curve given as Fig. 21(e)

We have seen that the non-linearity of the spatial filtering process prevents us from accurately achieving the required characteristic. It is by no means certain, however, that any filter profile can

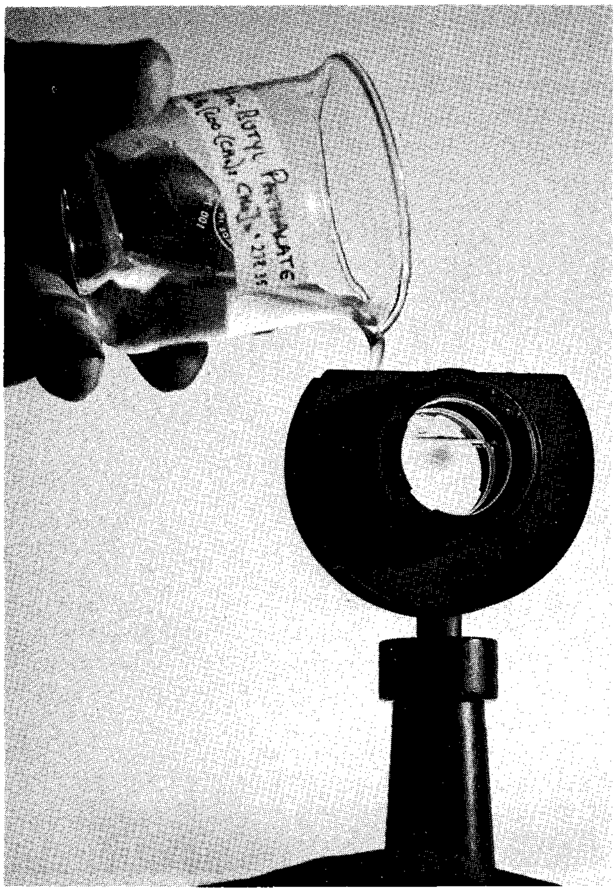

Fig. 24 - Liquid cell containing filter having a gradual change in opacity

be found which will have a characteristic sufficiently close to that desired if the light source is required to be as large as that used in the arrangement considered. This is because a profile designed to have a predominantly high-pass response/frequency characteristic for some of the elementary source points will inevitably have a low-pass component as seen from other source points. It is therefore desirable that the source be reduced in size. This reduction should, however, be made without prejudice to the photometric brightness at the negative, and it may be (see footnote on p. 8) that the latter is already insufficient. The difficulties would be increased if some light were to be lost in a splitting arrangement incorporated to allow individual control of the exposure of three colour–film photosensitive layers. The instrumentation would be complicated somewhat if three lasers (one red, one green, one blue) were used, but these would be ideally suited to a spatial filtering process. The source image would then be extremely small, and the characteristic of a spatial filter would be given immediately by its amplitude transmission profile. The colour separation effects, however, (see Section 3.2.3) which were negligible in the arrangement till now considered, would be increased if laser light were used, and some means of compensating for them might be necessary.

It is desirable whilst improving the reproduction of the higher spatial frequency components transmitted within the television pass-band to exclude from the positive print those which lie outside the transmitted band. These unwanted components may be at least attenuated by the use of an axial aperture positioned in the Fourier plane and of a size just sufficient to allow all of the wanted components to pass through. Such an aperture would also greatly reduce the veiling glare illustrated in Fig. 23.

6. CONCLUSIONS

Spatial filtering, applied to the printing process, appears to offer an attractive means of compensating for the loss of resolution that occurs in the production of colour film reduction prints. A simple arrangement for this purpose, using tungsten light passed through a pinhole as its illuminant, has been devised, and its properties have been investigated.

If in such an arrangement the pinhole is made large enough to obtain sufficient light at the image for a convenient exposure, the pinhole dimensions become comparable with the distances by which spatial frequency components are separated from each other at the Fourier plane. The filtering action is considerably complicated by the use of a finite sized source, and certain undesirable properties are introduced. A method of computing the response of a given filter under such circumstances has been devised and found to give good agreement with measured results. Further calculations and measurements will be made to determine the effect of filters having a gradual rather than an abrupt transition from transparency to opacity. It is believed that filters of this type will prove to have more suitable characteristics. It may be found, however, that the finite sources necessary to ensure an adequate exposure with tungsten illumination will not permit the required filtering to be made, in which case the use of lasers should be considered.

The gamma at which spatial filtering can be applied is different from that at which the loss of resolution occurs, but this is not expected to limit seriously the usefulness of the process. A printer incorporating spatial filtering would need to use a liquid gate, however, to remove the unwanted effects of surface and other irregularities. Care would need to be taken to reduce veiling glare within the optical system to a minimum.

7. REFERENCES

1. PORTER, A.B. 1906. On the diffraction theory of microscopic vision. *Phil. Mag.*, 1906, **11**, p. 159.

2. DUFFIEUX, P.M. 1946. L'integrale de Fourier et ses applications à l'optique. Rennes Société Anonyme des Imprimaries Oberthur, 1946.

3. O'NEILL, E.L. 1956. Spatial filtering in optics. *I.R.E. Trans. Inf. Theory*, 1956, June pp. 56 – 65.

4. Optical and electro optical information processing. M.I.T. Press,1965.

5. DOBRIN, M.B. et al. 1965. Velocity and frequency filtering of seismic data using laser light. *Geophysics*, 1965, **30**, 6, pp. 1144 – 1178.

6. MARECHAL, A. *and* CROCE, P. 1953. Une filtre de frequences spatiales pour l'amelioration du contraste des images optiques. *C.r.hebd. séanc. Acad.Sci., Paris*, **237**, pp. 607 – 609.

7. CROCE, P. 1956. Etude d'une methode de filtage des images optiques. *Revue Opt. théor. instrum.*, 1956, **35**, 11, pp. 569 – 589, and 12 pp. 642 – 656.

8. BORN, M. *and* WOLF, E. 1964. Principles of optics. London, Pergamon Press, 1964, p. 132.

9. Optical line broadening. BBC Research Department Report No. T-103, Serial No. 1963/13.

10. ZWICK, D. 1961. How colour negative film surface characteristics affect picture quality. *J. Soc. Motion Pict. Telev. Engrs.*, 1962, **71**, 1, pp. 15 – 20.

11. TURNER, J.R. et al. 1957. Printing motion-picture films immersed in a liquid; Part II – Optical printing. *J. Soc. Motion Pict. Telev. Engrs.*, 1957, **66**, 10, pp. 612 – 615.

12. BIRCH, K.G. A spatial filter to remove zero frequency. Optica Acta, 1968, **15**, 2, pp. 113 – 127.

*APPENDIX**

Modification of a Step Function by Sharp-Cut Filtering

Consider an amplitude distribution $G(x)$ defined by the equation

$$G(x) = H(x) - H(x - X) \qquad (1)$$

where $H(t)$ means Heaviside's unit-step function, zero for negative t and unity for positive t, and X is arbitrarily large and positive. Then $G(x)$ is zero when $x<0$ or $x>X$, and $G(x)$ is unity for $0<x<X$. The amplitude distribution at the Fourier plane is therefore given by

$$\Omega(\omega) = \int_{-\infty}^{\infty} G(x)e^{-i\omega x}dx = \int_{0}^{X} e^{-i\omega x}dx = j(e^{-i\omega X} - 1)/\omega \qquad (2)$$

Now suppose that the spatial filter removes from this spectrum the components between $\omega = -\omega_1$ and $\omega = \omega_2$ (ω_1, $\omega_2>0$). Then the resulting amplitude distribution at the image is given by

$$G'(x)=\frac{j}{2\pi}\left[\int_{-\infty}^{-\omega_1} e^{i\omega x}\left[\frac{e^{-i\omega X} - 1}{\omega}\right]d\omega + \int_{\omega_2}^{\infty} e^{i\omega x}\left[\frac{e^{-i\omega X} - 1}{\omega}\right]d\omega\right] \qquad (3)$$

$G'(x)$ in (3) can be expressed in terms of the tabulated sine and cosine integral functions Si(y) and Ci(y) defined by

$$\mathrm{Si}(y) = \int_0^y \frac{\sin t}{t}dt; \quad \mathrm{Ci}(y) = -\int_y^{\infty} \frac{\cos t}{t}dt = \int_{-\infty}^{-y} \frac{\cos t}{t}dt \qquad (4)$$

The integrand of Si(y) is indeterminate when $t = 0$ but tends to the limit 1 as t tends to zero, and Si(y) can therefore be regarded as a prefectly well-behaved *odd* function of y since its integrand is even. Ci(y), however, has a logarithmic infinity as $y \to 0$. But in dealing with (3) we are only concerned with *differences* involving Ci terms of the form Ci(ay) – Ci(by), and such differences can be regarded as well-behaved *even* functions of y. For it is well known that when y is positive

$$\mathrm{Ci}(y) = \log_e y + \gamma - \int_0^y \frac{1 - \cos t}{t}dt \qquad (5)$$

where γ is Euler's constant, defined by

$$\gamma = \lim_{n\to\infty} (1 + 1/2 + 1/3 + ... + 1/n - \log_e n) = 0{\cdot}577 \qquad (6)$$

and from this it can be shown that in all cases

$$\mathrm{Ci}(ay) - \mathrm{Ci}(by) = \log_e |a/b| + \int_{|ay|}^{|by|} \frac{1 - \cos t}{t}dt \qquad (7)$$

Hence in the case when ω_1 and ω_2 are positive, (3) reduces for sufficiently large X to

$$G'(x) = \frac{1}{2} - \frac{1}{2\pi}\left[\mathrm{Si}(\omega_1 x) + \mathrm{Si}(\omega_2 x)\right] + \frac{j}{2\pi}\left[\mathrm{Ci}(\omega_2 x) - \mathrm{Ci}(\omega_1 x)\right] \qquad (8)$$

whether x is positive or negative.

* This appendix was contributed by Mr. J.W. Head.

If the upper limit $-\omega_1$ of the first term in (3) becomes a positive quantity $+\omega_1$ instead of the negative quantity $-\omega_1$ hitherto assumed, the effect on $G'(x)$ is to add an extra term

$$F(\omega_1) = \frac{j}{2\pi}\int_{-\omega_1}^{\omega_1} e^{j\omega x}\left[\frac{e^{-j\omega X} - 1}{\omega}\right] d\omega \qquad (9)$$

and, again, the integrand of (9), though indeterminate, tends to a limit X when $\omega \to 0$. The odd part of the integrand contributes nothing, but the even part contributes for sufficiently large X

$$F(\omega_1) = -\frac{1}{\pi}\int_0^{\omega_1} \frac{\sin[\omega(x-X)] - \sin(\omega x)}{\omega}\, d\omega = \frac{1}{2} + \frac{1}{\pi}\mathrm{Si}(\omega_1 x) \qquad (10)$$

and a similar contribution $F(\omega_2)$ occurs if the lower limit ω_2 of the second term of (3) is replaced by $-\omega_2$, but since the spatial filter necessarily eliminates some frequency components, it is impossible to have both a contribution $F(\omega_1)$ and a contribution $F(\omega_2)$. We can, however, have one or other of these, or neither.

Thus if ω_1 and ω_2 are positive quantities, and the spatial filter eliminates components between $\omega = -\omega_1$ and $\omega = +\omega_2$ the amplitude distribution at the image is $G'(x)$ given by Equation (8) for either sign of x. If, however, the filter eliminates components between $\omega = +\omega_1$ and $\omega = \omega_2$ (where $\omega_1 < \omega_2$) the amplitude distribution at the image becomes $G''(x)$ where

$$G''(x) = G'(x) + F(\omega_1)$$

$$= 1 + \frac{1}{2\pi}\Big[\mathrm{Si}(\omega_1 x) - \mathrm{Si}(\omega_2 x)\Big] + \frac{j}{2\pi}\Big[\mathrm{Ci}(\omega_1 x) - \mathrm{Ci}(\omega_2 x)\Big] \qquad (11)$$

and if the filter eliminates components between $-\omega_1$ and $-\omega_2$ (where $\omega_1 > \omega_2$), the amplitude distribution becomes $G'''(x)$ where

$$G'''(x) = G'(x) + F(\omega_2)$$

$$= 1 + \frac{1}{2\pi}\Big[\mathrm{Si}(\omega_2 x) - \mathrm{Si}(\omega_1 x)\Big] + \frac{j}{2\pi}\Big[\mathrm{Ci}(\omega_1 x) - \mathrm{Ci}(\omega_2 x)\Big] \qquad (12)$$

By comparing expressions (8), (11) and (12), we see that the amplitude distribution at the image changes discontinuously when the sign of the highest or lowest spatial frequency eliminated by the filter changes, but changes continuously when the co-ordinate x (defining position in the image plane in Equation (3)) changes sign.

SMW

Printed by BBC Research Department, Kingswood Warren, Tadworth, Surrey